

SrRuO₃-SrTiO₃ heterostructure as a possible platform for studying unconventional superconductivity in Sr₂RuO₄

Bongjae Kim^{1,2,*}, Sergii Khmelevskiy³, Cesare Franchini^{4,5}, I. I. Mazin^{6,7}, and Kyoo Kim^{2,8,9†}

¹ Department of Physics, Kunsan National University, Gunsan, 54150, Korea

² MPPHC-CPM, Max Planck POSTECH/Korea Research Initiative, Pohang 37673, Korea

³ Center for Computational Materials Science, Institute for Applied Physics, Vienna University of Technology, Wiedner Hauptstrasse 8 - 10, 1040 Vienna, Austria

⁴ University of Vienna, Faculty of Physics and Center for Computational Materials Science, Vienna A-1090, Austria

⁵ Dipartimento di Fisica e Astronomia, Università di Bologna, 40127 Bologna, Italy

⁶ Code 6393, Naval Research Laboratory, Washington, DC 20375, USA

⁷ Quantum Materials Center, George Mason University, Fairfax, VA 22030, USA

⁸ Department of Physics, Pohang Institute of Science and Technology, Pohang 37673, Korea and

⁹ Korea Atomic Energy Research Institute (KAERI), 111 Daedeok-daero, Daejeon 34057, Korea

(Dated: June 4, 2020)

There is intense controversy around the unconventional superconductivity in strontium ruthenate, where the various theoretical and experimental studies suggest diverse and mutually exclusive pairing symmetries. Currently, the investigation is solely focused on only one material, Sr₂RuO₄, and the field suffers from the lack of comparison targets. Here, employing a density functional theory based analysis, we show that the heterostructure composed of SrRuO₃ and SrTiO₃ is endowed with all the key characteristics of Sr₂RuO₄, and, in principle, can host superconductivity. Furthermore, we show that competing magnetic phases and associated frustration, naturally affecting the superconducting state, can be tuned by epitaxial strain engineering. This system thus offers an excellent platform for gaining more insight into superconductivity in ruthenates.

Introduction. Transition metal oxides have long been a fertile ground for novel physics. In particular, unconventional superconductivity, found, for instance, in cuprates and ruthenates, is one of the most intriguing discovery of recent decades, and the physics and mechanisms in these oxides is still highly debated. The latter compound is particularly intriguing; despite tens of years of intensive studies, even a basic understanding of pairing symmetry is still lacking [1], and new surprises are continuously coming up. Arguably, one of the reasons the latter compound has been so difficult to crack is that it is a one-of-a-kind material. As opposed to the Cu- and Fe-based high- T_c superconductors, which have multiple families with many members each, Sr₂RuO₄ is a family of one, and no insightful comparison with any sibling can be effected.

In fact, one of the biggest breakthroughs in the field, which led to dramatic progress, occurred when experimentalists found a way to apply uniaxial strain so as to induce a Lifshitz transition [2, 3]. Finding another material, affording even more flexibility in modifying Sr₂RuO₄ properties, including its Fermiology and magnetic response, would open up a cornucopia of new experimental information and may lead to extraordinary progress in understanding the superconductivity in Sr₂RuO₄.

This idea is not new. Burganov *et al.* demonstrated that it is possible to grow epitaxial Sr₂RuO₄ thin films on a SrTiO₃ substrate, with a lattice mismatch of 0.9% [4]. No superconductivity was observed, which may be related to either too many defects at the interface (and the authors were optimistic about reducing their amount in the future), or due to a $\sqrt{2} \times \sqrt{2}$ reconstruction, also

present at the free-standing Sr₂RuO₄ surface. In particular, they observed in angle-resolved photoemission spectroscopy a Lifshitz transition not unlike the one seen under uniaxial strain, and speculated that approaching the van Hove singularity brings about a strong enhancement of the uniform magnetic susceptibility *via* the Stoner mechanism and therefore, strengthening of ferromagnetic (FM) spin fluctuations.

Very recently, such an enhancement has been observed in the resistivity [5], as well as in nuclear magnetic resonance (NMR) experiments and density functional theory (DFT) calculations [6] for bulk Sr₂RuO₄ under uniaxial stress. Note that, generally speaking, FM fluctuations favor triplet, and antiferromagnetic fluctuations favor singlet pairing. In the unstrained Sr₂RuO₄, the spin fluctuation spectrum is well documented [7], and it has been demonstrated that, barring other triplet-favoring interactions, the antiferromagnetic fluctuations win hands down. Yet, if pairing is indeed triplet, superconductivity which cannot benefit directly from the increased density of states (DOS) at the van Hove singularity can be boosted by these FM fluctuations, in accordance with the observed T_c behavior [3].

Not unexpectedly, the work by Burganov *et al.* [4] has triggered several works based on theoretical modelling employing tight-binding models [8, 9]. Unfortunately, such models do not take into account all the complexity of the epitaxial interface, band effects, and structural delicacy, and an extension to other systems has not been made so far. Here, we exploit the idea of heterostructures, employing first principles calculations, which, differently from model-based approaches, have a capacity

to capture much of the aforementioned complexity.

Curiously, while the cuprates, which are already a rather rich family, have been subjected to multiple suggestions and attempts to generate similar materials, including engineered heterostructures[10–18], Sr_2RuO_4 , which needs expansion onto other systems much more badly, has hardly been discussed in this context. Yet, from the perspective of the growth technique, epitaxy and heterostructuring are well-understood for ruthenates, especially for SrRuO_3 [19]. Particularly promising would be a superlattice composed of a single layer of SrRuO_3 sandwiched between insulating layers, which is now experimentally accessible with fine control [20–22]. It has the same principal structural motif as Sr_2RuO_4 , a two-dimensional square RuO_2 lattice. As we show below, it shares with Sr_2RuO_4 key features of the electronic structure and magnetic properties, but also has interesting and promising distinctions.

In the following, we report a first principles computational study of the electronic structure and magnetic properties of the SrRuO_3 - SrTiO_3 (SRO-STO) heterostructure, grown on a STO substrate (we will also briefly discuss other potential substrate ranges). The role of substrate is to fix the lateral lattice dimensions, and, thus, to provide biaxial strain. We show that the SRO-STO superlattice has all the key characteristics of Sr_2RuO_4 , and would broaden the exploratory potential dramatically in regard to the superconductivity mechanism and pairing symmetry.

Result and discussion. The most important structural feature of Sr_2RuO_4 is the two-dimensional (2D) RuO_2 layer, spaced between SrO layers, where the corner-shared RuO_6 octahedra form a square net. This active layer can be artificially constructed by sandwiching a SRO monolayer between STO blocks as shown in Fig. 1 (a), where the out-of-plane Ru-O-Ru connectivity is broken due to the interspersed STO layers. A small in-plane octahedral rotation ($\sim 8.2^\circ$ for unstrained case) exists for this superlattice, which produces a $\sqrt{2} \times \sqrt{2}$ supercell reconstruction in the plane [20]. This reconstruction is not found for the pure bulk phase of Sr_2RuO_4 , but is observed at the surface, as well as in a Ca-doped system [23–25], reflecting the tendency for RuO_6 octahedra to rotate, if necessary to accommodate the geometrical constraints. Note that even with this octahedral rotation pattern, surface superconductivity has been observed in tunneling [26].

The structural similarity of the two systems is reflected in their electronic structures. In Fig. 1 (b), we plotted the orbitally resolved partial density of states (DOS) of Ru- d for both systems. Due to an octahedral crystal field splitting, the three t_{2g} orbitals (xy , yz and zx) share four electrons, and are responsible for the low-energy physics. The xy orbital forms a quasi-2D band, and a nearly circular Fermi surface (FS), usually labeled as γ , and the other orbitals form two quasi-1D bands, which, upon

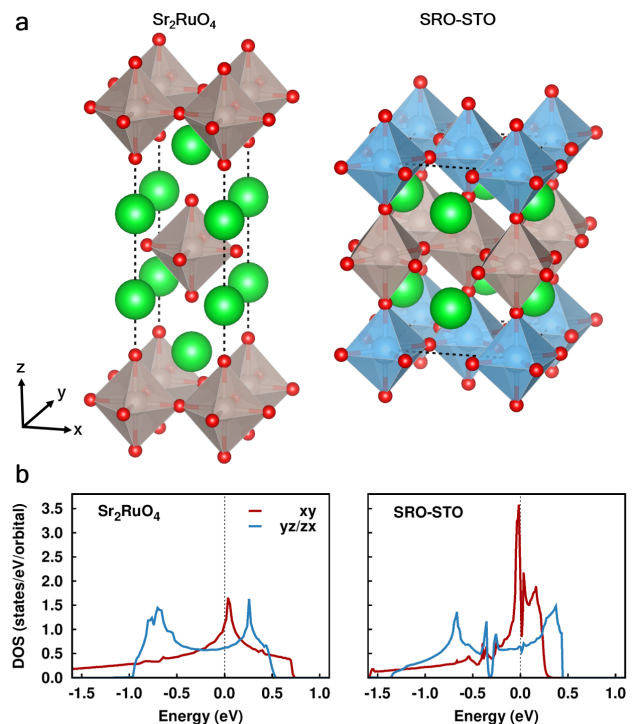


FIG. 1. (a) Crystal structure of Sr_2RuO_4 and SRO-STO. Gray and blue octahedra denote RuO_6 and TiO_6 octahedra, and red and green spheres represent oxygen and strontium atoms, respectively (b) Partial DOS of Ru- d orbitals for Sr_2RuO_4 and SRO-STO for xy and yz/zx .

intersection and re-hybridization, create two rounded-square shaped Fermi surfaces (α and β). From the partial DOS of SRO-STO, characteristic features observed in Sr_2RuO_4 are present as well. The peak of the xy partial DOS, corresponding to a 2D van Hove singularity (vHS), is located close to the Fermi level, and its contribution at the Fermi energy is much larger than those of the yz/zx bands. Less dispersive yz/zx orbitals have double-peak structures, corresponding to 1D vHS, and have smaller contributions at the Fermi level.

In Fig. 1 (b), one can notice that the xy DOS peak in the heterostructure is higher, and the bandwidth is smaller, than in Sr_2RuO_4 . This can be attributed to the octahedral rotations, which reduce the effective $xy - xy$ hopping as $\cos^2 \alpha$, where α is the rotational angle, while the $xz - xz$ and $yz - yz$ hopping is unaffected in the same order in α . This fact is immediately relevant for one of the main points of contention regarding superconductivity in Sr_2RuO_4 : while one school considers the xy band to have strong pairing, with superconductivity in xz/yz being induced by an interband proximity effect [27, 28], another advocates the xz/yz bands as the “active” subsystem, with xy being secondary [29]. Yet others suggested that all bands contribute roughly equally [30, 31]. Enhancing

selectively the DOS in the xy band only, through octahedral rotations (which, as we show later, can be controlled by the substrate), provides a direct test of these alternatives.

Another issue of relevance is the proximity to magnetism. It is well known that Sr_2RuO_4 is on the verge of an antiferromagnetic instability, driven by the quasi-1D nesting in the xz/yz bands. The corresponding spin fluctuations favor d -wave pairing [7, 31]. However, there is also, albeit a much weaker, tendency to a FM instability, which favors p -wave pairing. A dramatic increase in DOS brings the system much closer to ferromagnetism, thus strongly pushing the system toward a triplet pairing. Note that within the weak coupling limit, recent T_c enhancement in uniaxial strain experiment has been associated with odd- to even-parity transition, and our study can offer one way to verify this proposition [3].

With this in mind, we have looked at the magnetism of this system in more detail. Note that there have been DFT-based studies on SRO-STO system both in film and superlattices structures [22, 32–34], and they concluded the magnetic and electronic ground states of a single SRO layer to be either FM metal or Néel-type antiferromagnetic insulator. This issue is not also resolved as judged from the diverse experimental reports [20–22, 35]. The problem with these studies is that they take the DFT ground state at its face value, forgetting that it is, by nature, a mean-field approach, and, as such, liable to overestimate the tendency to magnetism. Indeed, straight DFT calculations predict Sr_2RuO_4 to be spin density wave (SDW) type antiferromagnetic (not a Néel-type, see below), and, with gradient corrections, even the FM state has lower energy than the nonmagnetic one [36]. This tendency can be corrected for, phenomenologically, by introducing the concept of a fluctuations-renormalized Stoner factor [37, 38], or strongly remedied by switching to dynamical mean field theory [39]. Applying the same concept to Sr_2RuO_4 and SRO-STO, we observed that the experimentally observed Stoner enhancement for the former is 7 [7], thus the Stoner product $IN(E_F) \approx 0.857$ [at the same time, renormalization at $\mathbf{q} = \mathbf{Q}_{\text{SDW}}$ is about 30, implying that $I(Q_{\text{SDW}})\chi_0(Q_{\text{SDW}}) \approx 0.967$, where χ_0 is bare susceptibility]. Our calculations find that the partial density of states of Ru orbitals on the Fermi level is about 50% higher in SRO-STO. This suggests that their $IN(E_F)$ is larger than one and the ground state should be FM. Fixed spin moment calculations confirm that in order to stabilize the paramagnetic state one would need to reduce the Stoner I by 3.5 times, which is completely unphysical.

As discussed below, the DOS at the Fermi level strongly depends on the epitaxial strain, which offers a unique opportunity to tune the system all the way from low DOS and low T_c to higher DOS and high T_c , as in the case of uniaxial strain [2, 3], and further to even higher DOS, *i.e.* the FM state. Furthermore, for a range

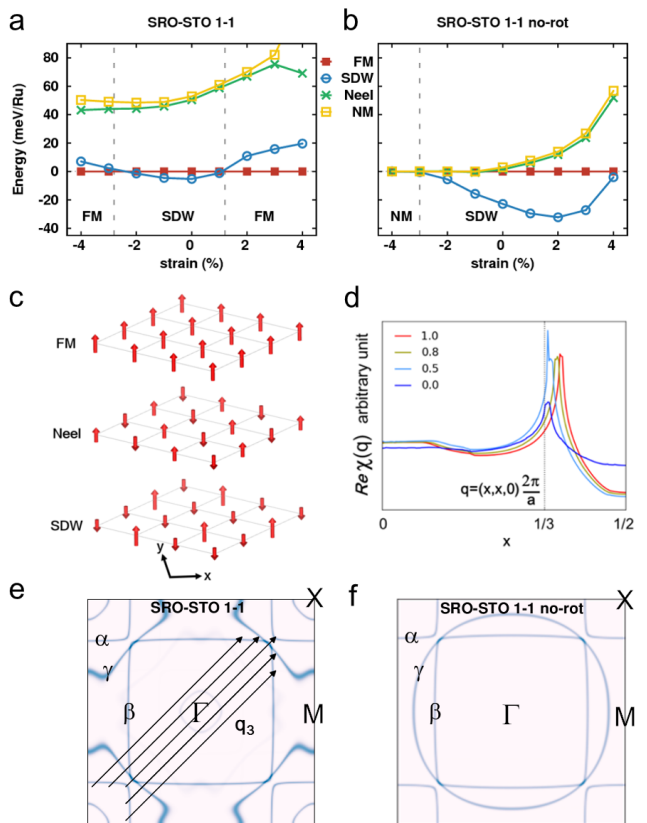


FIG. 2. The energy landscape as a function of strain (a) with and (b) without octahedral rotation of RuO_6 , for three magnetic configurations schematically depicted in (c): FM (ferromagnetic), Néel antiferromagnetic, and SDW ($\mathbf{q} = (1, 1, 0)\frac{2\pi}{3a}$) phases. (d) The change of Lindhard susceptibility obtained from the unfolded band for Ru yz/zx orbitals. Octahedral rotations are linearly interpolated between the unrotated case (0.0) and the fully rotated one (1.0). (e, f) The change of Fermi surfaces (e) with and (f) without octahedral rotation. (d)-(f) are for the unstrained (0%) structure. The arrows in the Fermi surfaces indicate \mathbf{q}_3 nesting vector which activates both the xz and yz quasi-1D-Fermi surfaces.

of strains the FM instability enters a fierce competition with the SDW one, which is even more enhanced for the SRO-STO system (See Fig. 2(a-c)). Bulk Sr_2RuO_4 is, both experimentally and theoretically, much closer to a SDW instability than to a FM one. Strong magnetic fluctuations have been observed by the neutron diffraction, which persists up to room temperature [40, 41]. This had been predicted in DFT studies [31] and a SDW with $\mathbf{q}_3 = (1, 1, 0)\frac{2\pi}{3a}$, a close commensurate approximation to the experimental peak in spin susceptibility, was shown to be stable in calculations [36, 42]. On the contrary, for the bulk material the FM state is barely stable in GGA, and unstable in LDA. There is no magnetic frustration in the system, with the SDW being a clear mean field ground state, suppressed by quantum fluctuations.

Interestingly, in SRO-STO, while both FM and SDW states gain stability, eventually they become nearly degenerate (Fig. 2(a) and (b)), adding a strong parametric frustration to the system. In a number of materials, most notably in Fe-based superconductors, such a strong magnetic frustration leads to complete destruction of a long-range magnetic order and numerous interesting phenomena, such as nematic order, and, arguably, superconductivity itself [43, 44]. It looks plausible that magnetic frustration in SRO-STO would prevent the system from developing a static magnetic order, but would trigger strong spin fluctuations, with all ramifications for the superconductivity. While the jury is still out on whether spin-fluctuation mechanism is instrumental in cuprates, Fe pnictides, or Sr_2RuO_4 , it is considered by many to be a strong contender in all three cases (which, of course, does not imply that the nature of superconductivity is the same in all three instances). Enhanced frustration of magnetism in SRO-STO, in this context, looks especially interesting.

Previous computational studies of SRO-STO superlattice concentrated upon the competition between FM and Néel orders [32, 34], ignoring the the SDW $\mathbf{q}_3 = (1, 1, 0)\frac{2\pi}{3a}$ phase. Our calculations show that, in spite of a dramatic stabilization of the FM phase, the SDW still has a lower energy (Fig. 2(a)) over a large range of strains (the Néel order is not competitive at all). The enhanced competition between the two magnetic phases in SRO-STO is promoted by the octahedral rotations, which are absent in Sr_2RuO_4 . As shown in Fig. 2 (b), the calculations with suppressed octahedral rotations favor the SDW tendency over FM. For strains between $\sim -2\%$ and $\sim 1\%$, the SDW has the lowest energy, but the energy gain is minimal, ~ 5 meV/Ru for zero strain case (the corresponding value for Sr_2RuO_4 is ~ 20 meV/Ru). For larger strains ($\lesssim -2\%$ and $\gtrsim 1\%$), the FM state becomes the most stable one. Note that the critical strain for the transition from SDW to FM is within the accessibility of current experimental techniques [45], and even broader epitaxial strain ranges could be reached in recent experiments [46]. This suggests that the SRO-STO system is a suitable platform for the control of different types of magnetic interactions, and, by implication, for tuning the superconducting order parameter. Note that, given that the fluctuation-induced suppression of magnetism may be, and probably is, \mathbf{q} -dependent, it is hard to say which state has the lowest free energy for which strain.

As can be seen in Fig. 2(d), the real part of the charge susceptibility in the SRO-STO system (see Supplementary Materials [47]) shows only a gradual shift of the \mathbf{q}_3 peak upon octahedral rotation. This is consistent with the fact that the α/β FSs remain quasi-one dimensional, with the same \mathbf{q}_3 nesting vector, as indicated by arrows in Fig. 2 (e). This lets us conclude that the antiferromagnetic SDW fluctuations are highly robust against octahe-

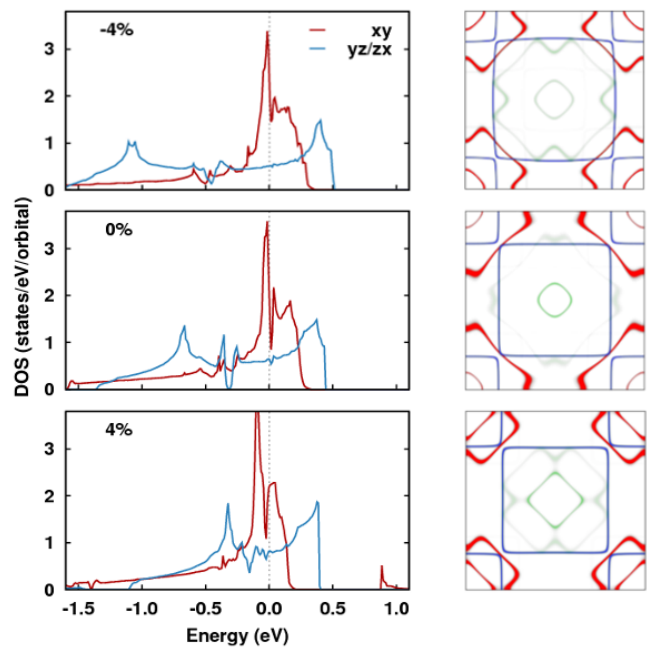


FIG. 3. Partial DOSs of Ru xy (red) and Ru yz/zx (blue) bands for strains -4% , 0% , and 4% . Corresponding Fermi surfaces including the Γ point are shown in the right column with the same color code. The contribution of other orbitals at Fermi surface is marked by the green color.

dral rotation, and, consequently, against substrate engineering. However, the two-dimensional γ FS is highly sensitive to octahedral rotations, which can be efficiently tuned by epitaxial strain. In particular, γ FS changes its shape with strain from a circle to a rounded square, which is not related to the van Hove singularity often discussed in strain studies of Sr_2RuO_4 [2, 3, 6], but is due to mixing between the xy and $x^2 - y^2$ orbitals of neighboring Ru atoms as shown in Figs. 2(e,f). The hybridization between xy and $x^2 - y^2$ bands due to octahedral rotation is eventually responsible for the additional FSs at around the Γ and X point for SRO-STO (Fig. 2(e)) [47].

Changes of DOSs and FSs upon strain are shown in Fig. 3. The width of yz/zx DOS becomes smaller as the tensile strain increases, while the xy DOS is nearly unaffected except for a shift of the peak position toward lower energies. Notably, the peak, mainly from the xy orbital, which is thought to be closely related with the T_c enhancement of uniaxial strain case, progressively moves down away from the Fermi level for tensile strains while the yz/zx DOS gradually increases at the Fermi level [47, 48]. For Sr_2RuO_4 , octahedral distortion shifts the peak down [49], while in SRO-STO, a tensile strain, which generally relieves the distortion, has a similar effect.

This selective evolution of the xy and yz/zx orbital upon strain suggests that future experimental studies of the SRO-STO system can probe the “active” orbitals, im-

portant for superconductivity [27–29]. Furthermore, the heterostructural features of the SRO-STO system itself can restrict specific types of scattering, and, within this structural setup, some superconducting symmetries, such those with horizontal node lines, cannot survive. The DOS at the Fermi level, which is tunable in our setup, is closely related with T_c behavior for a singlet pairing, but not for a triplet one. Thus, the possibility of a specific pairing such as $d_{x^2-y^2}$, which is promoted by the enhancement of the DOS at the Fermi level, can be directly tested in the SRO-STO system. Being close relatives of the orphan superconductor Sr_2RuO_4 , SRO-STO superlattices offer a unique possibility to controllably tune the Fermi surface topology, magnetic interactions and the position of the van Hove peak, thus providing new avenues to probe the pairing symmetry of the ruthenates.

Conclusion. SRO-STO heterostructures present an electronic system in many aspects similar to the intriguing putative triplet superconductor, Sr_2RuO_4 , but also distinctly different. The important common motif is the presence of the three Fermi surfaces, representing three Ru orbitals, xy , yz and zx , with the first one exhibiting a van Hove singularity at or near the Fermi level. Moreover, the exact topology of the Fermi surfaces can be modified within a reasonable range by varying the substrate and thus exerting different epitaxial strains. An important difference from Sr_2RuO_4 is that SRO-STO appears, in general, more magnetic, and at the same time the tendency to ferromagnetism is enhanced much more strongly than to the SDW. In principle, three scenarios can be realized, all three interesting in their own way. First, the enhanced tendency to SDW could lead to an actual instability. Second, at least for some strains, the material may become FM. The third, and arguably the most interesting, alternative is that the near-degeneracy (on a mean field level) of the FM and the SDW state will lead to a very strong parametric magnetic frustration that will preclude either static order, but will greatly enhance both types of fluctuations. In this case, the system, if manufactured cleanly enough, is likely to become superconducting, possibly in the triplet channel (boosted by FM fluctuations), but the properties of this superconducting state may be even more different from the bulk Sr_2RuO_4 than the critically strained samples [3]. If the symmetry of the superconducting state in Sr_2RuO_4 is indeed triplet (which is, however, strongly questioned by recent NMR experiments [50, 51]), the critical temperature of SRO-STO may be dramatically higher, because of stronger fluctuations, than that of Sr_2RuO_4 .

* bongjae.kim@kunsan.ac.kr

† kyoo@kaeri.re.kr

[1] A. P. Mackenzie, T. Scaffidi, C. W. Hicks, and Y. Maeno,

- npj Quantum Materials **2**, 40 (2017).
- [2] C. W. Hicks, D. O. Brodsky, E. A. Yelland, A. S. Gibbs, J. A. N. Bruin, M. E. Barber, S. D. Edkins, K. Nishimura, S. Yonezawa, Y. Maeno, and A. P. Mackenzie, *Science* **344**, 283 (2014).
- [3] A. Steppke, L. Zhao, M. E. Barber, T. Scaffidi, F. Jerzembeck, H. Rosner, A. S. Gibbs, Y. Maeno, S. H. Simon, A. P. Mackenzie, and C. W. Hicks, *Science* **355** (2017), 10.1126/science.aaf9398.
- [4] B. Burganov, C. Adamo, A. Mulder, M. Uchida, P. D. C. King, J. W. Harter, D. E. Shai, A. S. Gibbs, A. P. Mackenzie, R. Uecker, M. Bruetzam, M. R. Beasley, C. J. Fennie, D. G. Schlom, and K. M. Shen, *Phys. Rev. Lett.* **116**, 197003 (2016).
- [5] M. E. Barber, A. S. Gibbs, Y. Maeno, A. P. Mackenzie, and C. W. Hicks, *Phys. Rev. Lett.* **120**, 076602 (2018).
- [6] Y. Luo, A. Pustogow, P. Guzman, A. P. Dioguardi, S. M. Thomas, F. Ronning, N. Kikugawa, D. A. Sokolov, F. Jerzembeck, A. P. Mackenzie, C. W. Hicks, E. D. Bauer, I. I. Mazin, and S. E. Brown, *Phys. Rev. X* **9**, 021044 (2019).
- [7] P. Steffens, Y. Sidis, J. Kulda, Z. Q. Mao, Y. Maeno, I. I. Mazin, and M. Braden, *Phys. Rev. Lett.* **122**, 047004 (2019).
- [8] Y.-T. Hsu, W. Cho, A. F. Rebola, B. Burganov, C. Adamo, K. M. Shen, D. G. Schlom, C. J. Fennie, and E.-A. Kim, *Phys. Rev. B* **94**, 045118 (2016).
- [9] Y.-C. Liu, W.-S. Wang, F.-C. Zhang, and Q.-H. Wang, *Phys. Rev. B* **97**, 224522 (2018).
- [10] R. Arita, A. Yamasaki, K. Held, J. Matsuno, and K. Kuroki, *Phys. Rev. B* **75**, 174521 (2007).
- [11] V. I. Anisimov, D. Bukhvalov, and T. M. Rice, *Phys. Rev. B* **59**, 7901 (1999).
- [12] J. Chaloupka and G. Khaliullin, *Phys. Rev. Lett.* **100**, 016404 (2008).
- [13] P. Hansmann, X. Yang, A. Toschi, G. Khaliullin, O. K. Andersen, and K. Held, *Phys. Rev. Lett.* **103**, 016401 (2009).
- [14] H. Watanabe, T. Shirakawa, and S. Yunoki, *Phys. Rev. Lett.* **110**, 027002 (2013).
- [15] Y. K. Kim, O. Krupin, J. D. Denlinger, A. Bostwick, E. Rotenberg, Q. Zhao, J. F. Mitchell, J. W. Allen, and B. J. Kim, *Science* **345**, 187 (2014).
- [16] J. Gawraczyński, D. Kurzydłowski, R. A. Ewings, S. Bandaru, W. Gadomski, Z. Mazej, G. Ruani, I. Bergenti, T. Jaroń, A. Ozarowski, S. Hill, P. J. Leszczyński, K. Tokár, M. Derzsi, P. Barone, K. Wohlfeld, J. Lorenzana, and W. Grochala, *Proceedings of the National Academy of Sciences* **116**, 1495 (2019).
- [17] E. B. Isaacs and C. Wolverton, *Phys. Rev. X* **9**, 021042 (2019).
- [18] D. Li, K. Lee, B. Y. Wang, M. Osada, S. Crossley, H. R. Lee, Y. Cui, Y. Hikita, and H. Y. Hwang, *Nature* **572**, 624 (2019).
- [19] G. Koster, L. Klein, W. Siemons, G. Rijnders, J. S. Dodge, C.-B. Eom, D. H. A. Blank, and M. R. Beasley, *Rev. Mod. Phys.* **84**, 253 (2012).
- [20] M. Gu, Q. Xie, X. Shen, R. Xie, J. Wang, G. Tang, D. Wu, G. P. Zhang, and X. S. Wu, *Phys. Rev. Lett.* **109**, 157003 (2012).
- [21] H. Boschker, T. Harada, T. Asaba, R. Ashoori, A. V. Boris, H. Hilgenkamp, C. R. Hughes, M. E. Holtz, L. Li, D. A. Muller, H. Nair, P. Reith, X. Renshaw Wang, D. G. Schlom, A. Soukiassian, and J. Mannhart, *Phys. Rev. X*

- 9, 011027 (2019).
- [22] S. G. Jeong, T. Min, S. Woo, J. Kim, Y.-Q. Zhang, S. W. Cho, J. Son, Y.-M. Kim, J. H. Han, S. Park, H. Y. Jeong, H. Ohta, S. Lee, T. W. Noh, J. Lee, and W. S. Choi, *Phys. Rev. Lett.* **124**, 026401 (2020).
- [23] R. Matzdorf, Z. Fang, Ismail, J. Zhang, T. Kimura, K. T. Y. Tokura and, and E. W. Plummer, *Science* **289**, 746 (2000).
- [24] A. Damascelli, D. H. Lu, K. M. Shen, N. P. Armitage, F. Ronning, D. L. Feng, C. Kim, Z.-X. Shen, T. Kimura, Y. Tokura, Z. Q. Mao, and Y. Maeno, *Phys. Rev. Lett.* **85**, 5194 (2000).
- [25] S.-C. Wang, H.-B. Yang, A. K. P. Sekharan, S. Souma, H. Matsui, T. Sato, T. Takahashi, C. Lu, J. Zhang, R. Jin, D. Mandrus, E. W. Plummer, Z. Wang, and H. Ding, *Phys. Rev. Lett.* **93**, 177007 (2004).
- [26] I. A. Firmo, S. Lederer, C. Lupien, A. P. Mackenzie, J. C. Davis, and S. A. Kivelson, *Phys. Rev. B* **88**, 134521 (2013).
- [27] D. F. Agterberg, T. M. Rice, and M. Sgrist, *Phys. Rev. Lett.* **78**, 3374 (1997).
- [28] Y. Yanase, T. Jujo, T. Nomura, H. Ikeda, T. Hotta, and K. Yamada, *Physics Reports* **387**, 1 (2003).
- [29] S. Raghu, A. Kapitulnik, and S. A. Kivelson, *Phys. Rev. Lett.* **105**, 136401 (2010).
- [30] I. I. Mazin and D. J. Singh, *Phys. Rev. Lett.* **79**, 733 (1997).
- [31] I. I. Mazin and D. J. Singh, *Phys. Rev. Lett.* **82**, 4324 (1999).
- [32] P. Mahadevan, F. Aryasetiawan, A. Janotti, and T. Sasaki, *Phys. Rev. B* **80**, 035106 (2009).
- [33] M. Verissimo-Alves, P. García-Fernández, D. I. Bilc, P. Ghosez, and J. Junquera, *Phys. Rev. Lett.* **108**, 107003 (2012).
- [34] L. Si, Z. Zhong, J. M. Tomczak, and K. Held, *Phys. Rev. B* **92**, 041108 (2015).
- [35] Y. J. Chang, C. H. Kim, S.-H. Phark, Y. S. Kim, J. Yu, and T. W. Noh, *Phys. Rev. Lett.* **103**, 057201 (2009).
- [36] B. Kim, S. Khmelevskiy, I. I. Mazin, D. F. Agterberg, and C. Franchini, *npj Quantum Materials* **2**, 37 (2017).
- [37] P. Larson, I. I. Mazin, and D. J. Singh, *Phys. Rev. B* **69**, 064429 (2004).
- [38] L. Ortenzi, I. I. Mazin, P. Blaha, and L. Boeri, *Phys. Rev. B* **86**, 064437 (2012).
- [39] F. B. Kugler, M. Zingl, H. U. R. Strand, S.-S. B. Lee, J. von Delft, and A. Georges, arXiv:1909.02389 (2019).
- [40] Y. Sidis, M. Braden, P. Bourges, B. Hennion, S. NishiZaki, Y. Maeno, and Y. Mori, *Phys. Rev. Lett.* **83**, 3320 (1999).
- [41] K. Iida, M. Kofu, N. Katayama, J. Lee, R. Kajimoto, Y. Inamura, M. Nakamura, M. Arai, Y. Yoshida, M. Fujita, K. Yamada, and S.-H. Lee, *Phys. Rev. B* **84**, 060402 (2011).
- [42] S. Cobo, F. Ahn, I. Eremin, and A. Akbari, *Phys. Rev. B* **94**, 224507 (2016).
- [43] I. I. Mazin, M. D. Johannes, L. Boeri, K. Koepnik, and D. J. Singh, *Phys. Rev. B* **78**, 085104 (2008).
- [44] J. K. Glasbrenner, I. I. Mazin, H. O. Jeschke, P. J. Hirschfeld, R. M. Fernandes, and R. Valení, *Nature Physics* **11**, 953 (2015).
- [45] A. Vailionis, H. Boschker, W. Siemons, E. P. Houwman, D. H. A. Blank, G. Rijnders, and G. Koster, *Phys. Rev. B* **83**, 064101 (2011).
- [46] D. G. Schlom, L.-Q. Chen, C.-B. Eom, K. M. Rabe, S. K. Streiffer, and J.-M. Triscone, *Annu. Rev. Mater. Res.* **37**, 589 (2007).
- [47] See supplement materials for (i) calculation details, (ii) susceptibility calculation, (iii) strain-dependent changes of structure and DOSs, and (iv) role of spin-orbit coupling on the Fermi surfaces, which includes Refs. [52–60].
- [48] For the detailed structure of the DOS peak at around Fermi level, more accurate treatments are needed. For example, see Luo *et al.* [6]. In current study, we focus on the general trends upon the substrate strain.
- [49] E. Ko, B. J. Kim, C. Kim, and H. J. Choi, *Phys. Rev. Lett.* **98**, 226401 (2007).
- [50] A. Pustogow, Y. Luo, A. Chronister, Y.-S. Su, D. Sokolov, F. Jerzembeck, A. P. Mackenzie, C. W. Hicks, N. Kikugawa, S. Raghu, E. D. Bauer, and S. E. Brown, *Nature Physics* **574**, 72 (2019).
- [51] K. Ishida, M. Manago, and Y. Maeno, arXiv:1907.12236 (2019).
- [52] G. Kresse and J. Hafner, *Phys. Rev. B* **47**, 558 (1993).
- [53] G. Kresse and J. Furthmüller, *Phys. Rev. B* **54**, 11169 (1996).
- [54] J. P. Perdew, K. Burke, and M. Ernzerhof, *Phys. Rev. Lett.* **77**, 3865 (1996).
- [55] K. Koepnik and H. Eschrig, *Phys. Rev. B* **59**, 1743 (1999).
- [56] W. Ku, T. Berlijn, and C.-C. Lee, *Phys. Rev. Lett.* **104**, 216401 (2010).
- [57] M. E. Barber, F. Lechermann, S. V. Streltsov, S. L. Skornyakov, S. Ghosh, B. J. Ramshaw, N. Kikugawa, D. A. Sokolov, A. P. Mackenzie, C. W. Hicks, and I. I. Mazin, *Phys. Rev. B* **100**, 245139 (2019).
- [58] H. G. Suh, H. Menke, P. Brydon, C. Timm, A. Ramires, and D. F. Agterberg, arXiv:1912.09525 (2019).
- [59] K. M. Shen, A. Damascelli, D. H. Lu, N. P. Armitage, F. Ronning, D. L. Feng, C. Kim, Z.-X. Shen, D. J. Singh, I. I. Mazin, S. Nakatsuji, Z. Q. Mao, Y. Maeno, T. Kimura, and Y. Tokura, *Phys. Rev. B* **64**, 180502 (2001).
- [60] C. N. Veenstra, Z.-H. Zhu, B. Ludbrook, M. Capsoni, G. Levy, A. Nicolaou, J. A. Rosen, R. Comin, S. Kittaka, Y. Maeno, I. S. Elfimov, and A. Damascelli, *Phys. Rev. Lett.* **110**, 097004 (2013).

ACKNOWLEDGEMENTS

We thank Beom Hyun Kim and Minjae Kim for fruitful discussions. This work was supported by the NRF Grant (Contracts No. 2018R1D1A1A02086051 and 2016R1D1A1B02008461), the research funds of Kunsan National University, and Max-Planck POSTECH/KOREA Research Initiative (Grant No. 2016K1A4A4A01922028). The computing resources from the KISTI supercomputing center (Project No. KSC-2018-CRE-0079) is greatly acknowledged. I.I.M. acknowledges support by ONR through the NRL basic

research program.

Supplementary Material:
**SrRuO₃-SrTiO₃ heterostructure as a possible platform for studying
unconventional superconductivity in Sr₂RuO₄**

Bongjae Kim,^{1,2} Sergii Khmelevskiy,³ Cesare Franchini,^{4,5} I. I. Mazin,^{6,7} and Kyoo Kim^{2,8,9}

¹ *Department of Physics, Kunsan National University, Gunsan, 54150, Korea*

² *MPPHC-CPM, Max Planck POSTECH/Korea Research Initiative, Pohang 37673, Korea*

³ *Center for Computational Materials Science, Institute for Applied Physics, Vienna University of Technology,
Wiedner Hauptstrasse 8 - 10, 1040 Vienna, Austria*

⁴ *University of Vienna, Faculty of Physics and Center for Computational Materials Science, Vienna A-1090, Austria*

⁵ *Dipartimento di Fisica e Astronomia, Università di Bologna, 40127 Bologna, Italy*

⁶ *Code 6393, Naval Research Laboratory, Washington, DC 20375, USA*

⁷ *Quantum Materials Center, George Mason University, Fairfax, VA 22030, USA*

⁸ *Department of Physics, Pohang University of Science and Technology, Pohang 37673, Korea*

⁹ *Korea Atomic Energy Research Institute (KAERI), 111 Daedeok-daero, Daejeon 34057, Korea*

CALCULATION DETAILS

We performed *ab initio* electronic structure calculations using projector augmented wave method employing the Vienna *ab initio* simulation package (VASP) [52, 53], the generalized gradient approximation by Perdew-Burke-Ernzerhof with plane-wave cutoff of 400 eV [54]. For SRO-STO superlattice, we fixed in-plane lattice parameters to those of STO substrate, and varied strain up to 4% for tensile and compressive cases. Full atomic relaxation is performed for all cases, and Monkhorst-Pack k -mesh is used as corresponding to Ref. [36]. We also double checked the results with full potential local orbitals (FPLO) package [55] For the unfolding scheme and susceptibility calculation, we have utilized FPLO code.

SUSCEPTIBILITY CALCULATION

To compare the noninteracting susceptibility of SRO-STO with that of Sr₂RuO₄ on equal footing, we adopted the band-unfolding scheme of Ref. [56] to take into account of unit cell doubling induced by the octahedral rotations. The bare susceptibility of unfolded band for Ru $4d_{yz/zx}$ orbitals, a source of SDW fluctuation, is calculated as

$$Re\chi(q, \omega) = \sum_{a,b,b',k} \frac{A^{ab}(k, \omega)A^{ab'}(k+q, \omega)f^b(k)(1-f^{b'}(k+q))}{E_k^b - E_{k+q}^{b'} - \omega - i\delta},$$

where $A^{ab}(k)$ is the unfolded spectral weight, a corresponds to the bands in the unit cell without rotation (similar to that of Sr₂RuO₄). Here, $4d_{xy}$ and $4d_{xz}$ orbitals contribute to quasi-1D bands, and we only considered these bands, $a = \alpha, \beta$. b and b' are band indices of the supercell corresponding to the SRO-STO unit cell. When there is no octahedral distortion, the spectral weights for shadow bands vanish and the above equation describes the usual Lindhard susceptibility.

STRAIN-DEPENDENT DOS AND STRUCTURAL PARAMETERS

The strain dependence of the DOSs is shown in Fig. S1. As the strain evolves from compressive to tensile, the DOS at Fermi level, $N(E_F)$, changes strongly. The relative position of the van Hove peak barely changes for compressive strain ranging from -4% to 0%, but progressively moves away from the E_F for tensile strain regime. One should note that for a better description, a more exact treatment, as described in Ref. [6] is needed, which takes into account renormalization due to spin fluctuations. Also, electronic correlation and spin-orbit coupling will change some details of the van Hove peak[57], which are however not important for our paper.

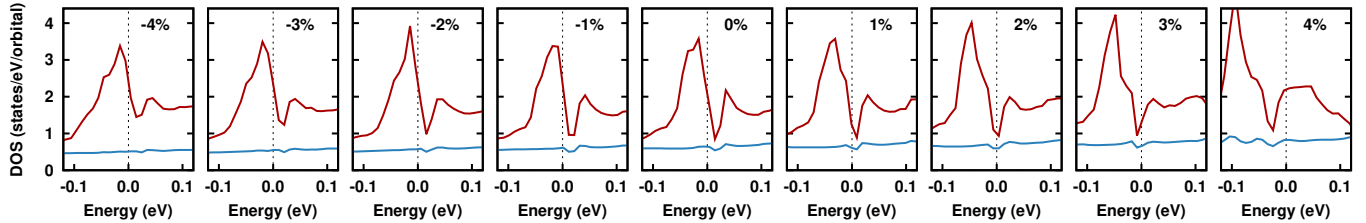


FIG. S1. The strain-dependent DOS evolution of xy (red) and yz/zx orbitals at around the Fermi level.

TABLE S1. Ru-O-Ru bond angle (α) and in-plane Ru-O bond length (d_{IP}) for different strains. Angles are in degrees ($^\circ$) and length scales are in (\AA)

strain	-4%	-3%	-2%	-1%	0%	1%	2%	3%	4%
α	11.3	10.4	9.5	8.7	8.2	8.1	7.7	7.3	8.5
d_{IP}	1.91	1.93	1.94	1.96	1.97	1.99	2.01	2.03	2.05

EFFECT OF SPIN-ORBIT COUPLING ON THE FERMI SURFACE

For SRO-STO, the overall effect of spin-orbit coupling on the FS is very similar to the case of Sr_2RuO_4 . In Fig. S2, we have compared the FSs with and without spin-orbit coupling. For the case without the octahedral rotation, the FSs show very similar characteristics of those from Sr_2RuO_4 (See Fig. S2(a) and (b)). The spin-orbit coupling does not change the overall shape of the FSs but shows clear splitting at the crossing point between β and γ sheets. This behavior is also observed with the inclusion of octahedral rotation (Fig. S2(c) and (d)). Despite the changes in the FSs are not spectacular, spin-orbit coupling can play an important role in deciding the superconducting ground states for Sr_2RuO_4 [58], and we believe that can be naturally applied to the case of SRO-STO. The effect of octahedral rotation and subsequent hybridization of the xy and $x^2 - y^2$ bands are reported for the surface of Sr_2RuO_4 [59, 60]. Similar effects are essentially observed in SRO-STO case, other than the details of the band morphology and occupations.

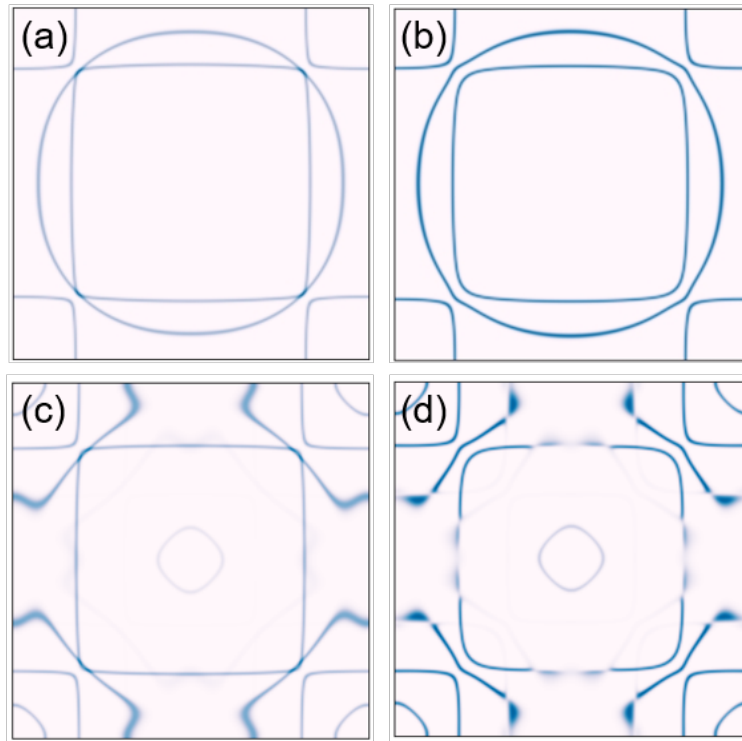


FIG. S2. The FSs of SRO-STO in the absence of octahedral rotation (a) without and (b) with the consideration of spin-orbit coupling. (c) and (d) are unfolded FSs with and without spin-orbit coupling, respectively, when the octahedral rotation is present.